Lidar-based Estimation of Turbulence Intensity for Controller Scheduling

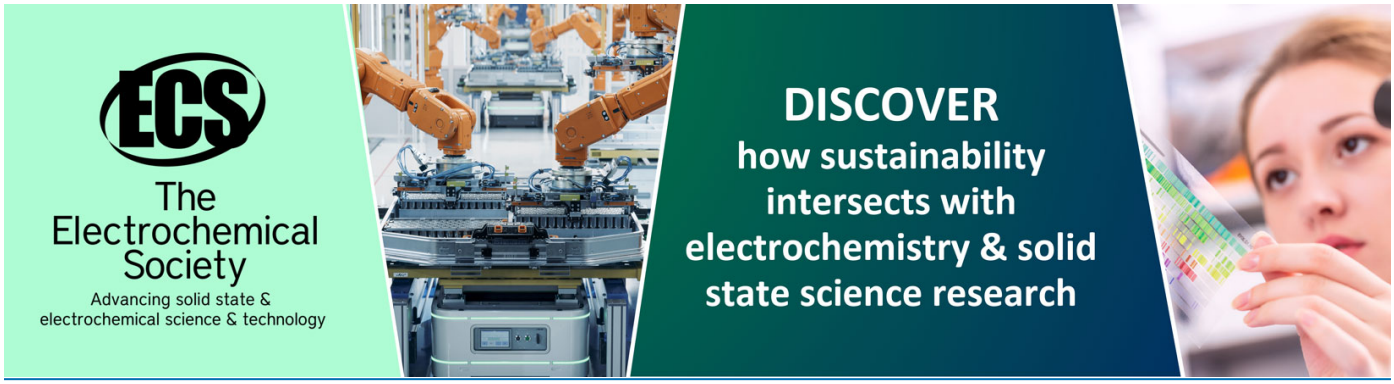

Lidar-based Estimation of Turbulence Intensity for Controller Scheduling

David Schlipf[1], Feng Guo[1], Steffen Raach[2]

[1] Flensburg University of Applied Sciences, Flensburg, Germany
[2] sowento GmbH, Stuttgart, Germany

E-mail: David.Schlipf@HS-Flensburg.de
Keywords: Lidar, Turbulence Intensity, IEA Wind, Lidar-Assisted Control, Extreme Loads

Abstract. Lidar-assisted wind turbine control is a promising technology and various concepts have been developed. This paper aims to add another concept to the list by describing how turbulence intensity can be estimated and used for controller scheduling to reduce structural loads. The turbulence intensity estimation is applied to lidar data from aero-elastic simulations and good agreement with the turbulence intensity calculation from wind fields is obtained. Further, a controller scheduling scheme is proposed to adjust the power level based on the estimated turbulence intensity. In a first simulation study, the scheduling scheme is able to reduce the power and extreme loads on the tower during severe turbulence conditions while keeping a similar level of power production and fatigue loads for normal turbulent conditions.

1. Introduction

Lidar systems are able to provide very accurate values for wind speed and wind direction averaged over ten minutes for site assessment [6]. However, calculating Turbulence Intensity (TI) from the wind speed signal provided by a lidar system usually leads to unsatisfactory results due to the probe volume and effects such as the cross-contamination [17]. Recent research focuses on estimating the TI with sophisticated estimation techniques [18, 16, 15] for ground-based lidar systems. Good estimates for the TI are also obtained by post-processing data from nacelle-based lidar systems using the Mann spectral model [14, 7].

Further, lidar-assisted control based on the online estimation of the rotor-effective wind speed is promising to reduce tower loads [4, 19]. Other concepts aim on using online estimates of blade-effective wind speeds or wind shears to reduce loads on blades [8, 13]. The yaw misalignment estimate from a lidar system can also improve wind turbine power capture [9].

Since the TI level has a large impact on the structural loads of wind turbines, using an online estimate of the TI appears useful to reduce the loads for different turbulence levels. In this work, we investigate, how the TI can be estimated in aero-elastic simulations with a realistic lidar simulator over different averaging time periods. We then use an estimate over three minutes to schedule a feedback controller to reduce the power and extreme loads in simulations with the Extreme Turbulence Model (ETM) [10]. The scheduling keeps the power and fatigue loads at the baseline level in simulations with the Normal Turbulence Model (NTM). The estimation of the TI based on lidar signals is encapsulated into a Dynamic Link Library (DLL) such that it can be combined with a standard feedback controller DLL, which is important to simplify the certification of lidar-assisted control applications [20].

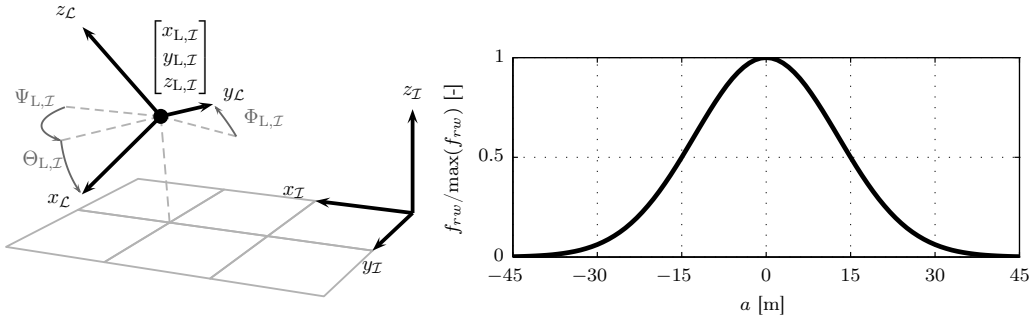

Figure 1. Left: Orientation of the lidar coordinate system (subscript $\mathcal{L}$) in the inertial coordinate system (subscript $\mathcal{I}$). Right: Normalized range weighting function for the used pulsed lidar system

2. Simulation Environment

In this section, the used wind turbine model, the lidar simulator, the selected lidar system and the coupling of the feedback controller and TI estimation are described. Further, the calculation of the TI from wind fields as a reference signal is presented.

2.1. IEA Wind Task 37 Reference Wind Turbine

In this work, the OpenFAST model of the 3.4 MW reference wind turbine from IEA Wind Task 37 [2] is used. The turbine has a rotor diameter of 130 m and a hub height of 110 m. The rated rotor speed is 11.75 rpm. A pitch actuator has been added in form of a second order linear model within the feedback controller DLL with the values from [2].

2.2. Lidar Simulator

The OpenFAST lidar simulator is an extension of OpenFAST developed at the University of Stuttgart and sowento based on [22], which provides raw lidar data during an aero-elastic simulation by scanning the same wind field which is used for the simulation of the wind turbine.

The simulator works with uniform and Bladed-style turbulent wind. When calculating the line-of-sight wind speeds, it takes into account the motion of the nacelle to which the lidar is assumed to be attached (see Figure 1). Furthermore, volume measurements are simulated by applying an user-defined weighting function to multiple measurements near a single focal point. The lidar simulator can be configured like any other OpenFAST module by modifying an input file. The input file allows the customization of the position and orientation of the lidar on the nacelle, the measurement ranges and beam directions as well as the range weighting function. In general, a lidar system is only able to measure the component of the wind vector in the laser beam direction. Therefore, the line-of-sight wind speed v_{LOS} measured by a stationary lidar system can be modeled by a projection of the wind vector $[u_{\mathcal{I}}\ v_{\mathcal{I}}\ w_{\mathcal{I}}]^T$ on the normalized vector of the laser beam $[x_{\mathrm{B},\mathcal{I}}\ y_{\mathrm{B},\mathcal{I}}\ z_{\mathrm{B},\mathcal{I}}]^T$. This is mathematically equivalent to the scalar product of both vectors:

$$v_{\mathrm{LOS}} = x_{\mathrm{B},\mathcal{I}} u_{\mathcal{I}} + y_{\mathrm{B},\mathcal{I}} v_{\mathcal{I}} + z_{\mathrm{B},\mathcal{I}} w_{\mathcal{I}}. \tag{1}$$

Further, real lidar systems measure within a probe volume. The volume measurement is modeled by a range weighting function f_{RW} depending on the distance a to the measurement point. For the pulsed lidar system considered in this work, a normalized Gaussian shape weighting function is used, (see Figure 1), following [5] with a pulse width at half maximum of 30 m. Finally, the

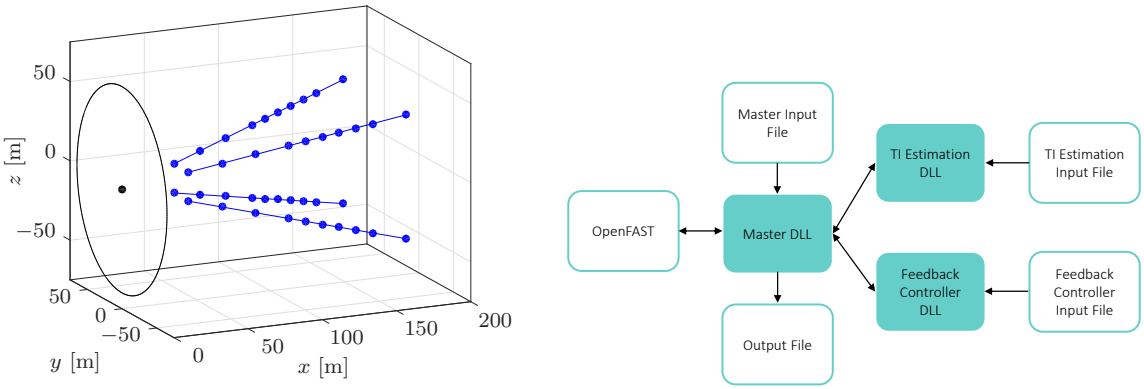

Figure 2. Left: Sketch of the scan pattern of the selected lidar system. Right: Structure of the DLL communication for OpenFAST.

line-of-sight wind speed is modeled by

$$v_{\mathrm{LOS}} = \int_{-\infty}^{\infty} \left(x_{\mathrm{B},\mathcal{I}} u_{a,\mathcal{I}} + y_{\mathrm{B},\mathcal{I}} v_{a,\mathcal{I}} + z_{\mathrm{B},\mathcal{I}} w_{a,\mathcal{I}}\right) f_{\mathrm{RW}}(a)\,\mathrm{d}a, \tag{2}$$

where $[u_{a,\mathcal{I}} v_{a,\mathcal{I}} w_{a,\mathcal{I}}]$ is the wind vector evaluated along the laser beam.

During aero-elastic simulations, the lidar simulator calculates the lidar states (position, velocity, and inclination) based on the current turbine states. The line-of-sight wind speeds v_{LOS} are then calculated using Equations (2), the lidar states, and applying Taylor's Hypothesis of Frozen Turbulence [23], which assumes that turbulent wind travels with the mean wind speed from the measurement location to the rotor.

2.3. Selected Lidar System

For this work, a commercial pulsed lidar system is used. The scan trajectory is illustrated in Figure 2. Table 1 summarizes the lidar configuration. The lidar is able to take measurements in several vertical planes.

Following data is then provided to the lidar data processing: line-of-sight wind speed v_{LOS} for each measurement distance, a flag for new measurements, the beam ID (0 to 3), similar to a real lidar system. With the current version of the lidar simulator[1], no blade impact or low availability can be simulated, thus a quality flag for each line-of-sight wind speed need to be added in a future version. The interface will be explained in the following subsection, the lidar data processing in the next section.

2.4. sowento DLL-Chain

The OpenFAST ServoDyn module, which allows the configuration of the turbine controller, supports a single external Bladed-style controller DLL. To process the lidar data from the lidar simulator, one approach would be to compile a single controller, which carries out all desired steps, such as lidar data-processing, feedforward control and feedback control. Here, a DLL-chain is used, consisting of a master DLL, which can be configured to sequentially call multiple secondary DLLs. This allows the encapsulation of individual control steps into separate DLLs. Figure 2 illustrates how the DLLs and their input files are connected: At every controller step,

[1] commit 829511a on 13 March 2020, `https://github.com/sowentoDavidSchlipf/openfast/tree/f/lidarsim`

Table 1. Selected scan configuration for the selected lidar system.

Number of beams	4
Beam azimuth-angles	15.0°, 15.0°,−15.0°,−15.0°
Beam elevation-angles	12.5°, −12.5°, −12.5°, 12.5°
Measurement distance	40, 60, 80, 100, 110, 120, 130, 140, 150, 170 m
Full scan time	1.0 s
pulse width at half maximum	30 m

OpenFAST calls the master DLL and passes the swap array. This array is the central part of the Bladed interface for external controllers [3]. Here, the master DLL merely passes on this array to all secondary DLLs. The master DLL and every sub-DLL have their own input file, which allows the configuration of the DLL behavior. Furthermore, the master DLL writes selected signals from all DLLs to an output file. For this work, the DLL-chain consists of DLLs for TI estimation and feedback control. The TI estimation DLL reads the raw lidar data, which has been written into the swap array by the lidar simulator. Based on this, it calculates an estimate of the rotor-averaged turbulence intensity and stores it in the array. The feedback DLL then reads the TI estimate and other turbine signals and returns the demanded torque and the demanded blade pitch angle.

2.5. Turbulence Intensity Calculation from Wind Fields

By definition, turbulence intensity is the standard deviation of the wind speed divided by the average wind speed over a certain averaging time period (typically 10 minutes) and at one point or a small volume [10], e.g. the turbulence measured by a cup anemometer (for horizontal wind) or by a ultra sonic anemometer (for all three components, i.e. longitudinal, lateral, vertical). It is an important measure for loads acting on a wind turbine. However, a single point is less representative for the whole rotor swept area. For control applications, a shorter averaging time period T can be beneficial. In this work, the rotor-averaged turbulence intensity $\mathrm{TI_R}$ of the longitudinal component at the current step k is calculated by

$$\mathrm{TI_R} = \frac{\frac{1}{n_\mathrm{p}} \sum_{i=1}^{n_\mathrm{p}} \sigma_{u,i}}{\overline{u}}, \tag{3}$$

where n_p is the number of wind speed points inside the rotor disk, $\sigma_{u,i}$ is the standard deviation of longitudinal wind speed of point i at step k, and $\overline{u}$ is the rotor average wind speed at step k. Here, $\overline{u}$ and $\sigma_{u,i}$ are obtained respectively by

$$\overline{u} = \frac{1}{n_\mathrm{p}} \sum_{i=1}^{n_\mathrm{p}} \overline{u}_i \quad \text{with} \quad \overline{u}_i = \frac{1}{n_\mathrm{t}} \sum_{j=k-n_\mathrm{t}+1}^{k} u_i \tag{4}$$

and

$$\sigma_{u,i} = \sqrt{\frac{1}{n_\mathrm{t}-1} \sum_{k=k-n_\mathrm{t}+1}^{k} (u_i - \overline{u}_i)^2}, \tag{5}$$

in which u_i is the longitudinal wind speed of point i at step k, $\overline{u}_i$ is the mean wind speed at point i over the averaging time period and n_t corresponds to the number of time steps in the averaging time period.

3. Lidar Data Processing

In this section, the TI estimation method is presented and evaluated.

3.1. Turbulence Intensity Estimation from Lidar Data

Similar to [14, 7], wind speed spectra and a frequency model of the lidar measurements are used to estimate the rotor-averaged turbulence intensity. Here, the IEC Kaimal spectral wind model [10] is used to calculate the spectrum $S_{\mathrm{los},ij}$ of each line-of-sight wind speed from range gate j and beam i using Equation (2) including the measurement volume of a pulsed lidar system and the current estimated wind direction following [21]. The variance of the line-of-sight signal for a averaging time period T can calculated by

$$\sigma_{\mathrm{L}}^2 = \int_{f_{\mathrm{min}}}^{f_{\mathrm{scan}}} S_{\mathrm{los},ij}\mathrm{df}, \tag{6}$$

where $f_{\mathrm{scan}} = 1\,\mathrm{Hz}$ is the measurement rate for each point and the minimum frequency f_{min} corresponds to $\frac{1}{T}$. By this, the contribution of frequencies below f_{min} is neglected. Similarly, the variance of a single longitudinal wind speed is calculated by

$$\sigma_u^2 = \int_{f_{\mathrm{min}}}^{f_{\mathrm{max}}} S_u\mathrm{df}, \tag{7}$$

where f_{max} is the maximum frequency used to generate the wind field. Finally, a correction factor can be calculated for each wind speed, wind direction and measurement point by

$$c_{\mathrm{TI}} = \frac{\sigma_u}{\sigma_{\mathrm{L}}}. \tag{8}$$

In simulations, the standard deviation of each signal v_{los} over the averaging time period T is corrected with its c_{TI}. The lidar estimate $\mathrm{TI_L}$ is then calculated by the mean from all corrected standard deviations and the mean wind speed over all measurements similar to Equation (3).

The main differences to the approach in [7] is that here the estimation is simplified by the use of the IEC Kaimal spectra model instead of the Mann model. We also include the effect of yaw misalignment and the impact of different averaging time periods directly in Equation (6).

3.2. Comparison of Estimated and Calculated Turbulence Intensity

The approach is tested using a baseline feedback controller and the simulation environment described above. For this purpose, 1 h wind fields with NTM and ETM are generated using TurbSim [11] with different seeds. The ETM wind field is generated for wind class IEC IA for better illustration. The wind fields are then extended by an exact copy to allow simulations of exactly 1 h after the buffer of the TI estimation is filled. Note that using an averaging time period of 1 h would yield constant $\mathrm{TI_R}$ calculation and due to tower motion almost constant $\mathrm{TI_L}$ estimation over the full simulation based on Veer's Method [24] to generate wind fields.

First, simulations are performed with an averaging time period of 10 min for both wind fields. The rotor-effective TI is continuously calculated using Equation (3). Although the TI used for the 1 h NTM wind field is 17.6 % and for the 1 h ETM wind field is 24.6 %, the highest TI of the NTM wind field is above the lowest TI of the ETM wind field, see Figure 3. Thus, within the 1 h ETM wind field there exist a 10 min block which is less turbulent than the most turbulent 10 min block within the 1 h NTM wind field. The TI from the wind field is then compared to its lidar estimate. The standard deviation of the error in both cases is very small (below 0.426 %).

The simulation is repeated with an averaging time period of 3 min for both wind fields (NTM and ETM), see Figure 4. Again, the standard deviation of the error is relatively low (below 0.765 % for both wind fields). The 3 min averaging time period is used for the controller scheduling in the following section, since it allows to react faster to TI changes. However, further work should investigate, which averaging time period is most helpful.

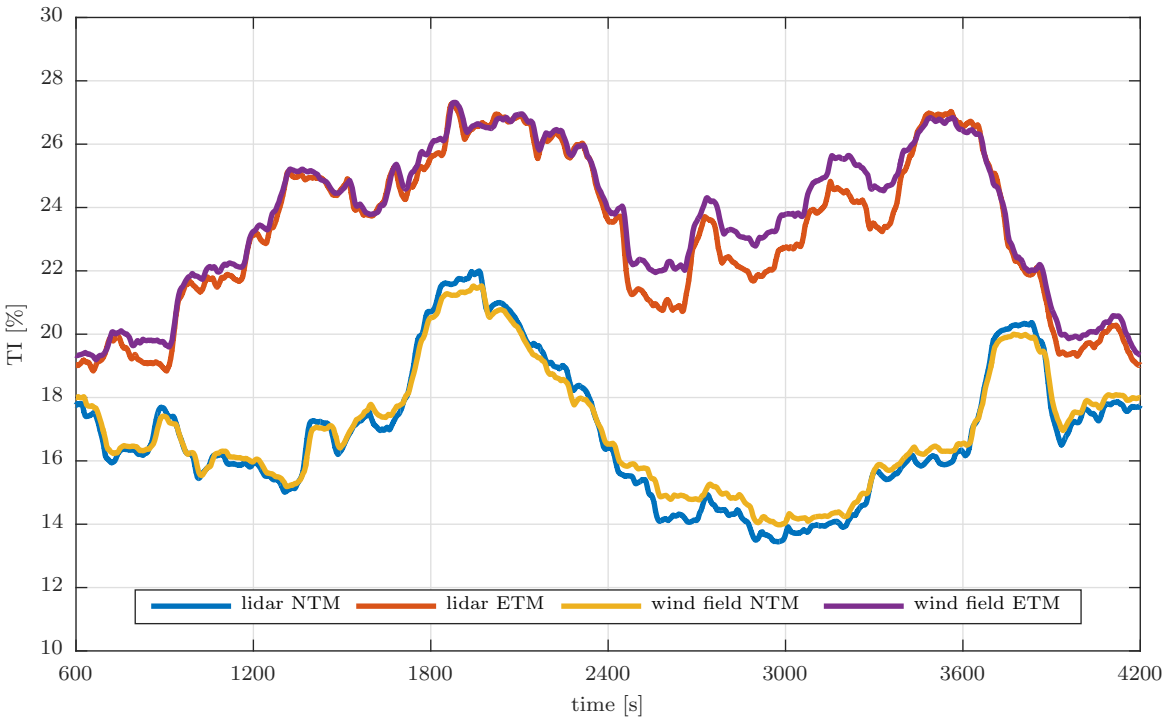

Figure 3. Comparision of a 10 min running calculation of TI from wind field and lidar estimate for normal and extreme turbulence level at a mean wind speed of 16 m/s.

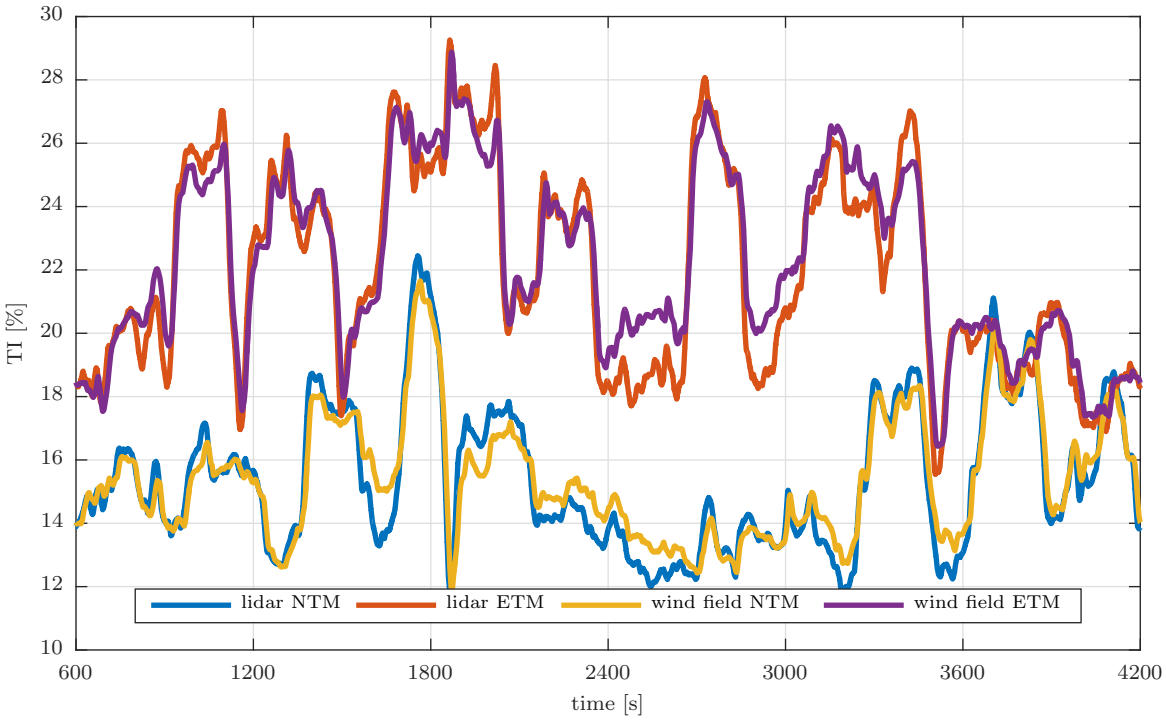

Figure 4. Comparision of a 3 min running calculation of TI from wind field and lidar estimate for normal and extreme turbulence level at a mean wind speed of 16 m/s.

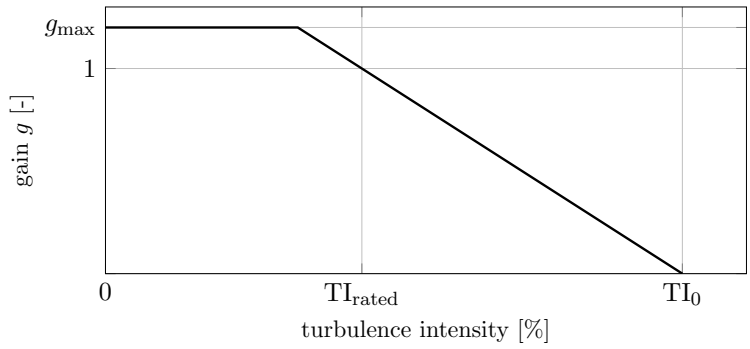

Figure 5. Controller Scheduling Scheme: gain depending on estimated turbulence intensity is used to schedule the power level.

4. Controller Scheduling

In this section, the baseline controller is briefly described. Then, the lidar-assisted power level scheduling is introduced.

4.1. Baseline Feedback Controller

The baseline feedback controller consists of a Proportional-Integral (PI) pitch controller and PI torque controller as well as a set-point-fading to coordinate pitch and torque controller[2]. The controller is close to industrial standard and has been optimized in above rated wind for fatigue load reduction. A similar approach has been used in [1]. In above rated wind conditions, the pitch controller tracks rated generator speed and the torque controller aims for constant power. The power level can be adjusted based on the TI estimate, see below. Further, the generator speed is filtered by a low pass filter and a notch filter at 3P (three times the rotational frequency).

4.2. Power Level Scheduling

The lidar-estimate of the TI is here used to schedule the feedback controller. In this work, the power level of the turbine is adjusted by a gain g depending on the current lidar TI estimate TI_L, see Figure 5. The gain is determined by 3 parameter: $\mathrm{TI}_{\mathrm{rated}}$, TI_0, and $g_{\max}$:

$$g = \frac{1}{\mathrm{TI}_{\mathrm{rated}} - \mathrm{TI}_0}\mathrm{TI}_\mathrm{L} - \frac{\mathrm{TI}_0}{\mathrm{TI}_{\mathrm{rated}} - \mathrm{TI}_0} \quad \text{s.t.} \quad 0 \leq g \leq g_{\max}. \tag{9}$$

Thus, rated power will be scheduled when the TI estimates equals to parameter $\mathrm{TI}_{\mathrm{rated}}$, and the gain reduces linearly after $\mathrm{TI}_{\mathrm{rated}}$ and finally is zero when turbulence intensity reaches TI_0. A maximum power lever is set by $g_{\max}$ to produce more electrical energy in less turbulent situations. The gain is multiplied with rated power and transferred to the torque controller, which adjusts the generator torque based on the power level and the generator speed.

Here, $\mathrm{TI}_{\mathrm{rated}}$=16% (close to mean of TI_R for T=3 min) and TI_0=32% have been chosen based on a brute force optimization for a mean wind speed of 16 m/s to keep the power and fatigue loads during the NTM simulation close to the baseline case (no scheduling) while reducing the maximum tower base bending moment during ETM simulations. The maximum power level is set to $g_{\max} = 1.1$ based on [12]. The results are presented in the next section. In future work, the parameters $\mathrm{TI}_{\mathrm{rated}}$ and TI_0 need to be further scheduled by the mean wind speed.

[2] Controller can be downloaded at `https://github.com/IEAWindTask37/IEA-3.4-130-RWT`

5. Simulation Results

In this section, the results from simulations with the extreme and normal turbulence model are presented. The results show that with the proposed TI estimation and power scheduling, the maximum tower base bending moment can be reduced during the ETM simulation at the cost of lower power while the power and fatigue loads are kept close to the baseline case during the NTM simulation.

5.1. Simulations with the Extreme Turbulence Model

First, the TI scheduled controller is compared to the baseline controller for the simulation with ETM. Figure 6 shows that the tower base bending moment can be significantly reduced, especially during periods with a high TI level (see Figure 4). In this simulation, the ultimate loads for the tower base bending moment are reduced from 87.5 MNm by 34.2% to 57.6 MNm. However, the mean power is reduced from 3.36 MW by 37.2% to 2.11 MW. The power loss is usually not considered during ETM simulations, e.g. in DLC 1.3 from [10].

5.2. Simulations with the Normal Turbulence Model

Second, the TI scheduled controller is compared to the baseline controller for the simulation with NTM. In Figure 7, no large impact on the tower loads can be seen. In NTM simulations, e.g. in DLC 1.2 from [10], fatigue loads are compared by calculating Damage Equivalent Loads (DELs). Here, the DELs for the tower base bending moment are calculated with a Wöhler exponent of 4 and a reference number of cycles of 2×10^6 and slightly increase from 84.0 MNm by 0.1% to 84.1 MNm. The mean power is also increased from 3.37 MW by 1.1% to 3.41 MW.

6. Conclusions and Further Work

In this work, a method is presented, which is able to provide an accurate estimation of the rotor-averaged turbulence intensity in aero-elastic simulations with a lidar simulator.

The estimated turbulence intensity is then used to adjust the power level of a baseline feedback controller in above rated wind conditions. With the proposed controller scheduling scheme, significant reduction in maximum tower base bending moment in extreme turbulent wind conditions is observed at the cost of lower power. With the same parameters, no large differences to the baseline controller for fatigue loads and mean power are observed in normal turbulent wind conditions.

Overall, the presented study indicates a good potential in extreme load reduction for the proposed concept. In this initial work, only simulations with a mean wind speed of 16 m/s are considered. A more detailed simulations study including a full DLC 1.2 and DLC 1.3 for IEC wind class IIIA (used for the turbine design), several turbulence seeds, and a load analysis of all components is necessary to access the potential under more realistic conditions. Further, the impact of the larger power fluctuations need to be investigated. For this purpose, a more sophisticated use of the TI estimate for the controller scheduling scheme should be also developed.

Also, TI scheduling of a combined feedback-feedforward controller will be considered in future work to fully exploit the information provided by the lidar technology. A real lidar system is subject to variable environment conditions. Thus, field testing is necessary to prove that this TI estimation and controller scheduling scheme is still beneficial under real conditions.

Finally, TI for power level scheduling could be also estimated based on turbine data, nacelle anemometers, direct calculations of TI from lidar signals or more complex methods [7]: thus, different estimation methods should be compared regarding their robustness, accuracy and applicability in wind turbine control and load verification.

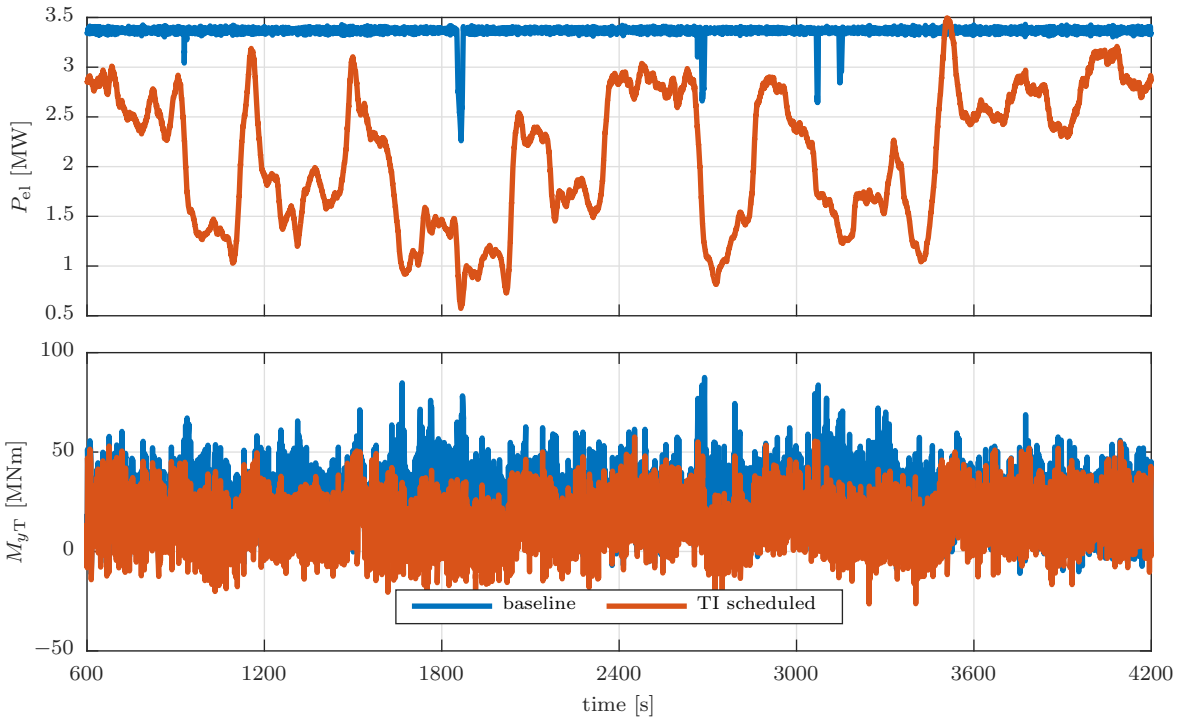

Figure 6. Comparision of baseline and TI scheduled simulations results with the extreme turbulence model at a mean wind speed of 16 m/s.

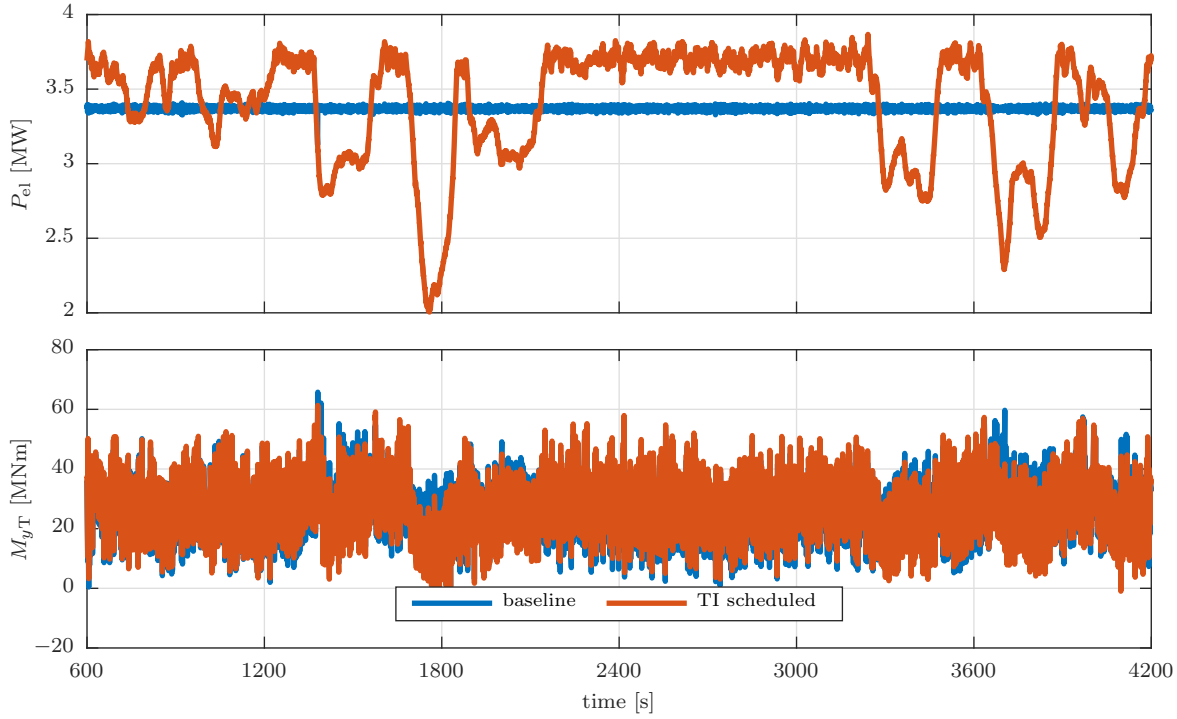

Figure 7. Comparision of baseline and TI scheduled simulations results with the normal turbulence model at a mean wind speed of 16 m/s.

Acknowledgment
This project has received funding from the European Union's Horizon 2020 research and innovation programme under the Marie Skłodowska-Curie grant agreement No. 858358 (LIKE – Lidar Knowledge Europe).

References
[1] Nikhar J. Abbas, Lucy Pao, and Alan Wright. An update to the national renewable energy laboratory baseline wind turbine controller. In *Journal of Physics: Conference Series*, 2020.
[2] Pietro Bortolotti, Helena Canet Tarres, Katherine Dykes, Karl Merz, Latha Sethuraman, David Verelst, and Frederik Zahle. IEA wind task 37 on systems engineering in wind energy – WP2.1 reference wind turbines. Technical report, International Energy Agency, 2019.
[3] Ervin Bossanyi. *GH Bladed Version 3.85 User Manual*, 2010.
[4] Ervin Bossanyi, Avishek Kumar, and Oscar Hugues-Salas. Wind turbine control applications of turbine-mounted lidar. *Journal of Physics: Conference Series*, 555(1):012011, 2014.
[5] Jean-Pierre Cariou. Pulsed lidars. In *Remote Sensing for Wind Energy, DTU Wind Energy-E-Report-0029(EN)*, chapter 5, pages 104–121. June 2013.
[6] Andrew Clifton, Peter Clive, Julia Gottschall, David Schlipf, Eric Simley, Luke Simmons, Detlef Stein, Davide Trabucchi, Nikola Vasiljevic, and Ines Würth. IEA wind task 32: wind lidar identifying and mitigating barriers to the adoption of wind lidar. *Remote Sensing*, 10(3):406, March 2018.
[7] Nikolay Dimitrov, Antoine Borraccino, Alfredo Peña, Anand Natarajan, and Jakob Mann. Wind turbine load validation using lidar-based wind retrievals. *Wind Energy*, 22(11):1512–1533, 2019.
[8] Fiona Dunne, David Schlipf, Lucy Y Pao, A D Wright, Bonnie Jonkman, Neil Kelley, and Eric Simley. Comparison of two independent lidar-based pitch control designs. In *Proceedings of the 50th AIAA Aerospace Sciences Meeting Including the New Horizons Forum and Aerospace Exposition*, 2012.
[9] P A Fleming, A K Scholbrock, A Jehu, S Davoust, E Osler, A D Wright, and A Clifton. Field-test results using a nacelle-mounted lidar for improving wind turbine power capture by reducing yaw misalignment. *Journal of Physics: Conference Series*, 524(1):012002, 2014.
[10] IEC 61400-1. Wind turbines - Part 1: Design requirements, 2005.
[11] B. J. Jonkman. TurbSim user's guide. Technical Report TP-500-46198, NREL, 2009.
[12] J. Jonkman, S. Butterfield, W. Musial, and G. Scott. Definition of a 5-MW reference wind turbine for offshore system development. Technical Report TP-500-38060, NREL, 2009.
[13] Knud Abildgaard Kragh, Morten Hartvig Hansen, and Lars Christian Henriksen. Sensor comparison study for load alleviating wind turbine pitch control. *Wind Energy*, 17(12):1891–1904, 2014.
[14] A. Peña, J. Mann, and N. Dimitrov. Turbulence characterization from a forward-looking nacelle lidar. *Wind Energy Science*, 2(1):133–152, 2017.
[15] Alfredo Peña and Jakob Mann. Turbulence measurements with dual-doppler scanning lidars. *Remote Sensing*, 11:2444, 10 2019.
[16] Lucie Rottner, Christophe Baehr, Alain Dabas, and Linda Hammoud. Stochastic method for turbulence estimation from Doppler lidar measurements. *Journal of Applied Remote Sensing*, 11(4):1 – 22, 2017.
[17] A. Sathe, R. Banta, L. Pauscher, K. Vogstad, D. Schlipf, and S. Wylie. Estimating turbulence statistics and parameters from ground- and nacelle-based lidar measurements. Technical report, International Energy Agency, October 2015.
[18] A. Sathe, J. Mann, N. Vasiljevic, and G. Lea. A six-beam method to measure turbulence statistics using ground-based wind lidars. *Atmospheric Measurement Techniques*, 8(2):729–740, 2015.
[19] David Schlipf. *Lidar-Assisted Control Concepts for Wind Turbines*. PhD thesis, University of Stuttgart, 2015.
[20] David Schlipf, Nikolai Hille, Steffen Raach, Andrew Scholbrock, and Eric Simley. IEA Wind Task 32: Best Practices for the Certification of Lidar-Assisted Control Applications. *Journal of Physics: Conference Series*, 1102:012010, oct 2018.
[21] David Schlipf, Jakob Mann, and Po Wen Cheng. Model of the correlation between lidar systems and wind turbines for lidar assisted control. *Journal of Atmospheric and Oceanic Technology*, 30(10):2233–2240, 2013.
[22] David Schlipf, Juan José Trujillo, Valeria Basterra, and Martin Kühn. Development of a wind turbine LIDAR simulator. In *Proceedings of the European Wind Energy Conference*, Marseille, France, 2009.
[23] G. I. Taylor. The spectrum of turbulence. *Proceedings of the Royal Society of London. Series A - Mathematical and Physical Sciences*, 164(919):476–490, 1938.
[24] Paul S. Veers. Three-dimensional wind simulation. Technical Report SAND88-0152, Sandia National Laboratory, 1988.